

Selena Mimmi, Anna Maria Zimbo, Salvatore Rotundo*, Erika Cione, Nancy Nisticò, Annamaria Aloisio, Domenico Maisano, Anna Maria Tolomeo, Vincenzo Dattilo, Rosaria Lionello, Antonella Fioravanti, Antonio Di Loria, Angela Quirino, Nadia Marascio, Alessandro Russo, Enrico Maria Treçarichi, Giovanni Matera, Ileana Quinto, Carlo Torti and Enrico Iaccino*

SARS CoV-2 spike protein-guided exosome isolation facilitates detection of potential miRNA biomarkers in COVID-19 infections

<https://doi.org/10.1515/cclm-2022-1286>

Received October 26, 2022; accepted February 24, 2023;

published online March 27, 2023

Abstract

Objectives: Nearly three years into the pandemic, SARS-CoV-2 infections are occurring in vaccinated and naturally infected populations. While humoral and cellular responses in COVID-19 are being characterized, novel immune biomarkers also being identified. Recently, an increase in angiotensin-converting enzyme 2 expressing (aka, ACE2 positive) circulating exosomes (ExoACE2) were identified in the plasma of COVID-19 patients (El-Shennawy et al.). In this pilot study, we describe a method to characterize

the exosome-associated microRNA (exo-miRNA) signature in ACE2-positive and ACE2-negative exosomal populations (non-ExoACE2).

Methods: We performed a sorting protocol using the recombinant biotin-conjugated SARS CoV-2 spike protein containing the receptor binding domain (RBD) on plasma samples from six patients. Following purification, exo-miRNA were characterized for ACE2-positive and ACE2-negative exosome subpopulations by RT-PCR.

Results: We identified differential expression of several miRNA. Specifically let-7g-5p and hsa-miR-4454+miR-7975 were upregulated, while hsa-miR-208a-3p and has-miR-323-3p were downregulated in ExoACE2 vs. non-ExoACE2.

Conclusions: The SARS CoV-2 spike-protein guided exosome isolation permits isolation of ExoACE2 exosomes. Such purification facilitates detailed characterization of potential biomarkers (e.g. exo-miRNA) for COVID-19 patients. This method could be used for future studies to further the understanding mechanisms of host response against SARS CoV-2.

Selena Mimmi and Anna Maria Zimbo share first co-authorship.

Carlo Torti and Enrico Iaccino share the senior position.

***Corresponding authors: Salvatore Rotundo**, Department of Medical and Surgical Sciences, Magna Graecia University of Catanzaro, Catanzaro, Italy, E-mail: srotundo91@gmail.com; and **Enrico Iaccino**, Department of Experimental and Clinical Medicine, Magna Graecia University of Catanzaro, Catanzaro, Italy, E-mail: iaccino@unicz.it

Selena Mimmi, Anna Maria Zimbo, Nancy Nisticò, Annamaria Aloisio, Vincenzo Dattilo and Ileana Quinto, Department of Experimental and Clinical Medicine, Magna Graecia University of Catanzaro, Catanzaro, Italy

Erika Cione, Department of Pharmacy, Health and Nutritional Sciences, University of Calabria, Rende, CS, Italy

Domenico Maisano, Harvard Medical School, Boston, MA, USA

Anna Maria Tolomeo, Department of Cardiac, Thoracic and Vascular Science and Public Health, University of Padova, Padua, Italy

Rosaria Lionello, Alessandro Russo, Enrico Maria Treçarichi and Carlo Torti, Department of Medical and Surgical Sciences, Magna Graecia University of Catanzaro, Catanzaro, Italy

Antonella Fioravanti, Structural and Molecular Microbiology, Structural Biology Research Center, Brussels, Belgium

Antonio Di Loria, Department of Veterinary Medicine and Animal Productions, University Federico II of Napoli, Napoli, Italy

Angela Quirino, Nadia Marascio and Giovanni Matera, Clinical Microbiology Unit, Department of Health Sciences, Magna Graecia University of Catanzaro, Catanzaro, Italy

Keywords: ACE2; biomarkers; Covid19; exosomes; miRNAs.

Introduction

Despite the tremendous success of coronavirus disease 2019 (COVID-19) vaccine development, the continuous appearance of rapidly evolving genetic severe acute respiratory syndrome coronavirus 2 (SARS-CoV-2) variants makes paramount the identification of novel minimally invasive approaches for patient stratification, disease staging, and treatment regimen design. Indeed, even if COVID-19 disease moves toward endemicity with a considerable decrease in the daily average number of deaths, the persistent and cyclic transmission rate calls for fortified efforts to further characterize the viral pathogenesis and the related possible interventions [1].

Recently, El-Shennawy et al. reported an increase in circulating exosomes expressing ACE2 (ExoACE2) in the

plasma of COVID-19 patients, highlighting the potential role of a first-line immune response against viral infection [2]. Indeed, they reported the capability of ExoACE2 to bind the spike protein of SARS-CoV-2 virions and inhibit pneumocyte infection, both *in vitro* and *in vivo*, in murine models [2]. The authors speculated a direct physical involvement of these small extracellular vesicles (EVs) in suppressing access of SARS-CoV-2 to its host cell surface without providing a molecular explanation for the reported ExoACE2-mediated inhibition of SARS-CoV-2 infection. To explore potential mechanisms of inhibition, we examined the miRNA contents (aka, cargo) of ExoACE2 compared with that of non-ACE2-expressing exosomes (non-ExoACE2) in order to identify possible new biomarkers for immune response and clinical course prediction.

Due to their all-pervasive distribution within biofluids, exosomes are considered one of the most promising biomarker sources in liquid biopsy innovations [3]. The combination of their molecular composition and the diversity of cargos make these endosomal-originated nano-vehicles complex [4]. In particular, exosomes associated with pathological alterations could be mined to identify innovative biomarkers for longitudinal measures during disease progression [5]. Once released in biological fluids, exosomes migrate to target cells and, by direct contact, can release their content into them, thus influencing the cell target phenotype, metabolism, and intracellular pathways [6]. This process plays an intriguing role in the progression of several diseases, such as cancer [7], neurodegenerative diseases [8], and, as recently demonstrated, also in SARS-CoV-2 infection [2]. However, the challenge remaining for EV-devoted researchers is the characterization of single-cell exosomes, such as in physiological vs. pathological conditions [9, 10].

Several methods have been described for exosome purification that include differential centrifugation and detection of surface molecules such as CD81 and CD63 [11] vs. phage display technology [12, 13]. Of these two approached, the phage display approach was able to provide differential molecular characterization of the exosome associated miRNA (aka, exo-miRNA) cargo. Exo-miRNAs are small RNAs detectable through liquid biopsy. Exo-miRNA influence gene expression and thus playing an essential role in the pathogenesis of a wide range of diseases including regulating the immune response against infectious diseases [14, 15]. Because exo-miRNAs are protected within EVs, they are more resistant to degradation vs. circulating miRNA [16] and may be more stable as potential biomarkers.

Previously, we demonstrated that exo-miRNAs represent a diverse molecular cargo in terms of potential

biomarker resources [17]. In this pilot study, we applied our biomarker discovery approach to expand upon recent findings of El-Shennawy et al. [2] by differentially characterizing ExoACE2 and non-ExoACE2 and their respective exo-miRNA cargo in the context of SARS CoV-2 infection.

Materials and methods

Sample collection

Serum samples were collected from six COVID-19 patients in the acute phase of the disease (within 7 days following exposure). All patients were referred to the Infectious and Tropical Disease Unit of Magna Graecia University of Catanzaro, Italy. The research related to human use complied with all the relevant national regulations, institutional policies and was in accordance with the tenets of the Helsinki Declaration (revised in 2008) (World Medical 2013), and was approved by the authors' Ethical Committee (no.COVID19@UMG POR Calabria-FESR/FSE 2014–2020 D.D.R.C. n. 4584 del 4/5/2021-Azione 10.5.12). Informed consent was obtained from all individuals included in this study.

Purification of total exosomes from patients' serum

Exosomes were size exclusion-isolated from 500 μ L of serum using qEVoriginal/35 nm columns (Izon, Izon Science Ltd.) according to the manufacturer's protocol. The size distribution and concentration of EV particles were evaluated using the tunable resistive pulse sensing (TRPS) method (qNano, Izon Science Ltd.) and an NP100 nanopore membrane with 47.5 nm stretch. All measurements were calibrated using 110 nm polystyrene calibration beads appropriately diluted (CPC 100, Izon Science Ltd.) in the same measurement conditions. Sample analysis was carried out using Izon Control Suite software v3.3 (Izon Science, UK).

Physical characterization of purified exosomes

Dynamic light scattering and zeta potential were determined with a Nano ZS 90 (Malvern Instruments), allowing the analysis of particles within the range of 1 nm–3 μ m. For morphological investigation, COVID-related exosomes were fixed with 4% paraformaldehyde (PFA) for 5 min and one drop (10 μ L) of them was placed on a 400-mesh perforated film grid for 10 min. After washing with PBS, COVID-related exosomes were stained with 1% uranyl acetate for 2 min. Then, the sample was washed with PBS and finally observed with a Tecnai G2 (FEI) transmission electron microscope (TEM) operating at 100 kV. Images were captured with a Veleta digital camera (Olympus Soft Imaging System).

Isolation and validation of ExoACE2s from COVID-19 patients' serum

To verify the expression of ACE2 receptor by the previously purified exosomes, we first performed flow cytometry analysis (BD FACSCanto II) using an CD63 Exo-Flow capture kit (System Biosciences – SBI, Palo Alto, California, USA) following the manufacturers' instructions and as

previously reported [12]. Briefly, the CD63-conjugated beads were firstly incubated overnight (O.N.) with the previously isolated exosomes and secondly labeled with anti-ACE2 (Miltenyi Biotec, Bergisch Gladbach, Germany) (Figure 1A).

The exosome sorting protocol was performed using recombinant biotin-conjugated RBD spike viral protein (Sino Biological Europe GmbH, Eschborn, Germany) in combination with streptavidin-conjugated beads (Thermo Fisher, Waltham, Massachusetts, USA) following the manufacturers' instructions. Briefly, 100 μ L of streptavidin-conjugated beads was mixed with 0.4 μ g of the recombinant biotin-conjugated RBD spike viral protein and incubated for 1 h at room temperature. Tubes were placed on a magnet for 1 min, the supernatant was removed, and beads were washed with 1 mL of the supplied washing buffer. The conjugated beads were added to the previously isolated serum-released exosomes and incubated O.N. at 4 °C. The following day, tubes were placed on the magnet for 1 min and the supernatants containing the unbound exosomes were recovered as non-ExoACE2 samples (Figure 1B). To assess the validity of the sorting protocol, a small amount of non-ExoACE2 samples (100 μ L) was tested for the expression

of ACE2 using a CD63 Exo-Flow capture kit and an ACE2 antibody as detailed above (Figure 1C).

NanoString sample preparation and data analysis

For the nCounter flex of NanoString Technology, 50 ng of RNA/miRNA was used as input. Firstly, total miRNAs were extracted from exosomes using an exoRNeasy kit purchased from Qiagen (Hilden, Germany) according to the manufacturer's instructions. In detail, the annealing master mix was prepared by combining 13 μ L of annealing buffer, 26 μ L of nCounter miRNA tag reagent, and 6.5 μ L of the 1:500 miRNA assay controls dilution prepared as follows: 1 μ L of miRNA assay controls and 499 μ L of nuclease-free water. An aliquot of 3.5 μ L of the annealing master mix was placed into each tube of a 0.2 mL strip tube plus 3 μ L of RNA sample. The samples underwent the following thermal cycler conditions: 94 °C for 1 min, 65 °C for 2 min, 45 °C for 10 min. Following the finishing point of the annealing protocol, when the thermal cycler had reached 48 °C, 2.5 μ L of the ligation master mix was added to each tube.

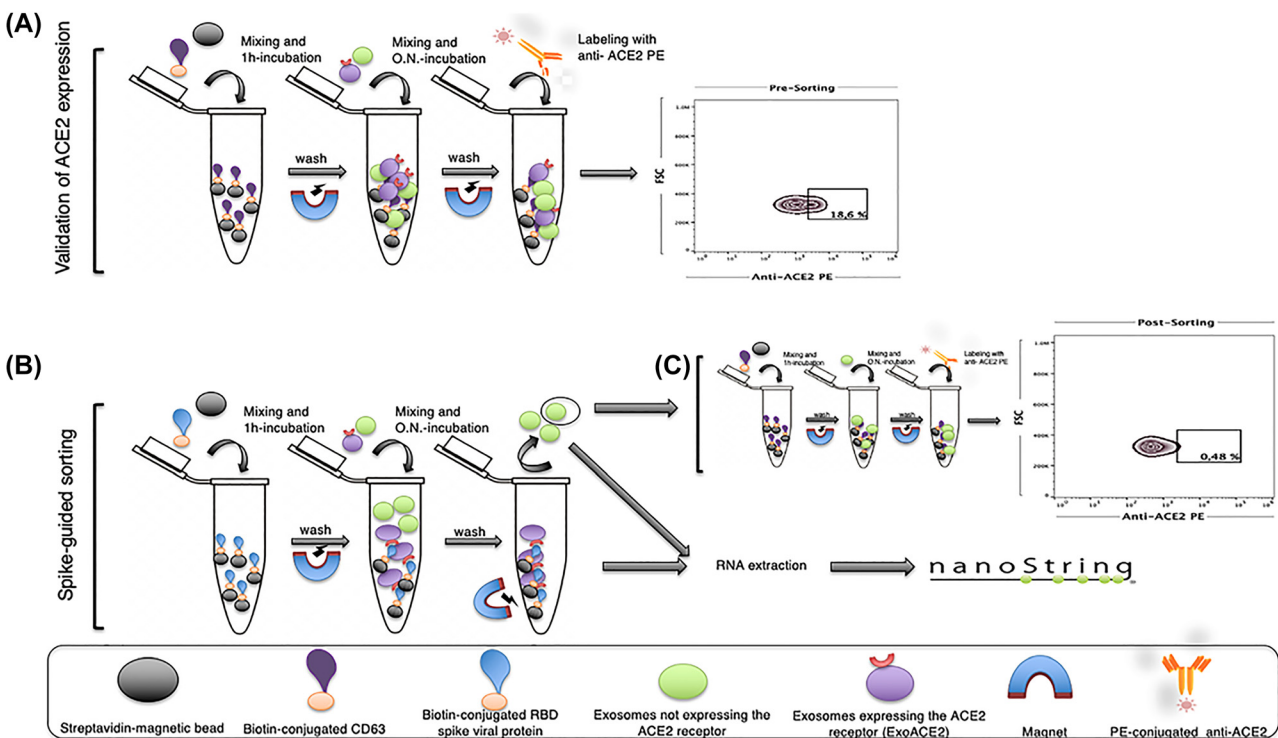


Figure 1: Workflow of the exosome sorting protocol. Graphical representation of the exosome sorting protocol. (A) Total exosomal population was tested for the expression of ACE2 before sorting. First, the streptavidin-conjugated beads (black circle) were coated with CD63 (purple drop) conjugated with biotin (orange circle). After 1 h of incubation and unbound washing, total exosomes were added and incubated overnight. CD63-positive exosomes were labeled with PE-conjugated anti-ACE2 and visualized by flow cytometry. A representative flow cytometry plot (pre-sorting) shows about 18% of ACE2 expressing exosomes of the total exosome population in the rectangular gate. (B) Exosomes were sorted using as bait the recombinant RBD spike viral protein. First, the streptavidin-conjugated beads (black circle) were coated with the recombinant RBD spike viral protein (blue drop) conjugated with biotin (orange circle). After 1 h of incubation, total exosomes representing ACE2-expressing exosomes (violet circle) and exosomes not expressing ACE2 (green circle) were added and incubated overnight (O.N.). After three cycles of washing, the two populations, unbound exosomes (exosomes not expressing ACE2, green) and bound exosomes (ExoACE2, violet), were separately recovered using a magnet and processed for RNA extraction and NanoString analysis. (C) A small amount of exosome preparations not expressing ACE2 (green circles) were analyzed by flow cytometry for the expression of CD63 and ACE2 using the same protocol as for plot A. Representative flow cytometry plot (post-sorting) shows the absence of ExoACE2 in the rectangular gate and the validity of the sorting protocol.

The ligation master mix was prepared by combining 22.5 μL of polyethylene glycol and 15 μL of ligation buffer to obtain a 15 \times solution. The strip was then flicked and spun down gently. The strip was returned to the 48 $^{\circ}\text{C}$ thermal cycler with the lid closed and incubated at 48 $^{\circ}\text{C}$ for 5 min. Maintaining the temperature at 48 $^{\circ}\text{C}$ is critical for optimal assay performance. Then 1 μL of ligase was added directly to the bottom of each tube to be sure that all samples received it having a dilution of 1:10. There is no need to mix. Immediately after the addition of ligase to the last tube, the tubes were recapped, and the thermal cycler lid was closed. The ligation protocol was started to have a species-specific tag sequence (miRtag) via a thermally controlled splinted ligation at 48 $^{\circ}\text{C}$ for 3 min, 47 $^{\circ}\text{C}$ for 3 min, 46 $^{\circ}\text{C}$ for 3 min, 45 $^{\circ}\text{C}$ for 5 min, and at 65 $^{\circ}\text{C}$ for 10 min. After finishing the ligation protocol, the unligated miRtags were removed by enzymatic purification by adding 1 μL of ligation clean-up enzyme to each tube to initiate the purification protocol with the following thermal cycler conditions: 37 $^{\circ}\text{C}$ for 60 min and 70 $^{\circ}\text{C}$ for 10 min. Then, the strip was removed from the heat block, and 40 μL of nuclease-free water was added to each sample, mixed well, and spun down.

Then, miR-tagged mature miRNAs were hybridized with a nCounter Human (V3) miRNA Expression Assay CodeSet following the manufacturer's instruction (code CSO-MIR3-12). The hybridization master mix was prepared by adding 130 μL of hybridization buffer to the tube containing 130 μL of reporter CodeSet. Then 20 μL of hybridization master mix was added to each tube of the strip containing the sample that was previously denatured at 85 $^{\circ}\text{C}$ for 5 min and then quick-cooled on ice. The addition of 5 μL of Capture ProbeSet was performed when the thermal cycler reached 65 $^{\circ}\text{C}$ to increase the assay's sensitivity. The hybridization reaction was performed for 36 h. The unhybridized CodeSet was removed by automated purification performed with a nCounter Prep Station to determine whether the remaining target probes' complexes were transferred and bound to an imaging surface. Counts of the reporter probes were tabulated for each sample using a nCounter Digital Analyzer. Each sample was scanned for 555 fields of view (FOV). The raw data output was imported into nSolver™ (<https://www.nanostring.com/products/analysis-software/nsolver>). Data were normalized by the first top 100 miRs, and statistical analysis was done according to the software instructions (<https://doi.org/10.1093/bioinformatics/bts188>). Then Excel normalized table data were exported, and t-test and logarithms were calculated to build the volcano plot. The volcano plot was created using GraphPad 8.0. It displays an unstandardized signal (\log_2 fold change) against a noise-adjusted/standardized signal ($-\log_{10}$ (p-value) from the t-test). The adjusted p-value was performed following the Benjamini–Hochberg (BH) procedure. The 95% confidence interval (CI) with upper and lower values was also calculated using the data analysis function in Excel.

Results

Starting from the serum of six patients in the acute phase of the disease Table 1 we used the recombinant RBD spike viral protein to purify the ExoACE2.

The workflow of the protocol for exosome sorting is represented in Figure 1. EVs presented a spherical shape with a diameter of approximately 50–120 nm and revealed the presence of the lipid bilayer. The physical analysis confirmed, therefore, that almost all the nanoparticles

isolated from our patients can be referred to as “small EVs” according to the MISEV2018 criteria [18] (Figure 2A and B). Following sorting, both populations (ExoACE2 and non-ExoACE2) were recovered. The reliability of our ExoACE2 sorting protocol was confirmed by flow cytometry, demonstrating the complete spike protein-dependent ACE2 depletion in the exosomal samples (Figure 3).

The differentially sorted EVs were processed for nucleic acid purification, and the resulting miRNAs were analyzed using an nCounter miRNA Expression kit. Interestingly, unsupervised hierarchical clustering showed that the exosomes sorted for their affinity to the RBD spike viral protein showed an independent exosome-derived miRNA profile. Among 800 miRNAs present in the commercially available panel nCounter miRNA-V3 screening the most biologically relevant miRNAs (updated to miRBase 22), in ExoACE2, we identified four deregulated exo-miRNAs with respect to the EVs not expressing ACE2, as reported in Table 2. In particular, let-7g-5p and hsa-miR-4454+miR-7975 were upregulated, while hsa-miR-208a-3p and has-miR-323-3p were downregulated in ExoACE2 vs. non ACE2 expressing exosomes (Figure 4).

Discussion

It has been demonstrated that miRNAs of the let-7 family act as immune response modulators and influence CD8-positive T-cell activation [19]. Moreover, two published works indicate that circulating let-7g-5p is associated with a better prognosis in COVID-19 disease and can interact with the SARS-CoV-2 genome and negatively influence replication and infection [20, 21]. Another miRNA of the let7 family, has-let7b-5p, has recently been observed to be deregulated in nasopharyngeal swabs from COVID-19 patients; it modulates the expression of ACE2 and DPP4, enforcing the hypothesis of an essential role of these miRNAs in SARS-CoV-2 infection [22]. Interestingly, hsa-miR-208a-3p has been described to be associated with myocyte injuries, so it could be a predictor of heart damage in COVID survivors [23].

While future studies are needed, with the presented data, we speculate the ability of ExoACE2 to influence the miRNA-driven immune response against SARS-CoV-2 infection. Although the active role of EVs in the most various pathological states is not well investigated, exosomes would seem to polarize the signals related to the immune system in a virus-neutralizing way, as indicated by the activation of CD8-positive T cells by the miRNA let-7g-5p contained in the ExoACE2 cargo [24].

These new shreds of evidence show a promising and novel use of exosomes as biomarker sources and immune

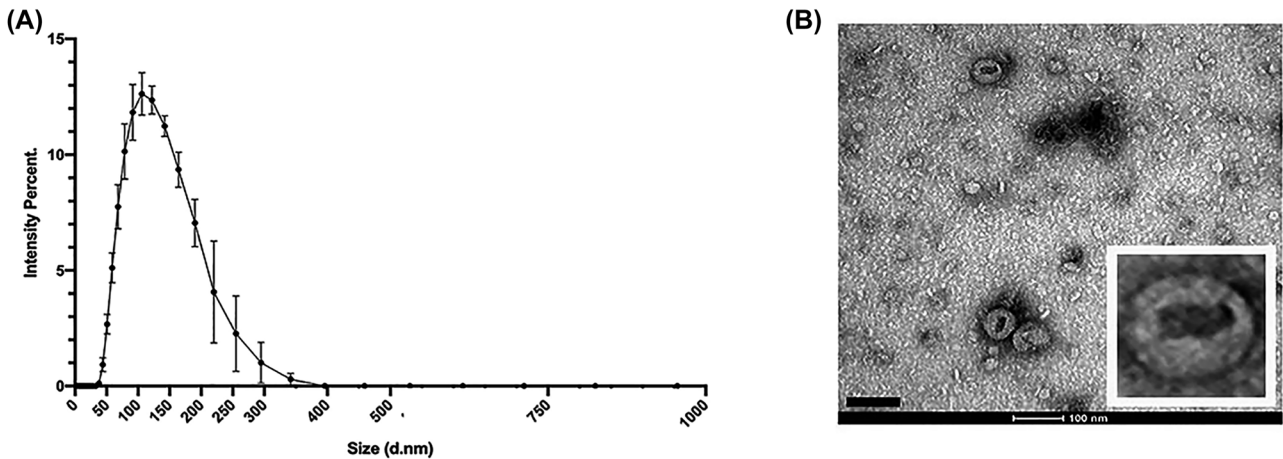


Figure 2: Physical and molecular characterization of isolated ACE2-expressing exosomes. The isolated nanoparticles were physically characterized using dynamic light scattering (Zetasizer Nano S, Malvern Instruments) (A) and transmission electron microscopy (scale bar=100 nm; insert shows a higher-magnification image) (B). Both analyses confirmed that all isolated vesicles can be referred to as “small EVs”, according to the MISEV2018 criteria [18].

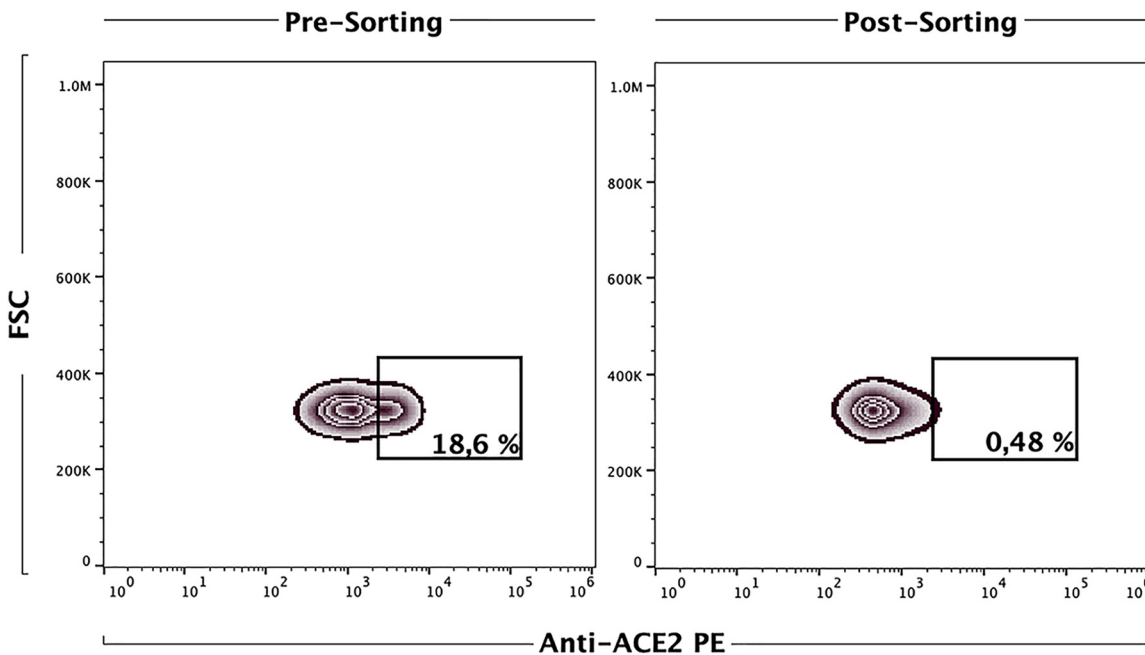


Figure 3: Representative image of flow cytometry analysis of isolated exosomes pre- and post-RBD spike-based sorting. Comparing the two plots, it is possible to appreciate the complete depletion of ACE2-expressing exosomes after sorting (from 18.6 to 0.48%).

interactors, with an active role in virus neutralization. In this scenario, our validated method for exosome subpopulation isolation, trapping, and characterization offers a promising future platform that can be used in the context of other infectious diseases. In addition, validation of the identified deregulated miRNAs could be adopted in a more representative cohort of subjects, including both vaccinated and unvaccinated patients, as well as responders and non-responders. Such evidence could be of help in the

development of liquid biopsy tests devoted to the effective monitoring of immune response in the course of the infection and could open up crucial advances in terms of patient-specific and timely appropriate booster vaccination programs.

Acknowledgments: The authors thank Prof. Giuseppe Novelli, Prof. Pasquale De Bonis, Prof. Andrea Morandi and Prof. Rossella Russo for their valuable comments, suggestions

Table 1: Clinical data of enrolled patients.

Characteristic	Patient 1	Patient 2	Patient 3	Patient 4	Patient 5	Patient 6
Gender	Female	Male	Female	Female	Male	Female
Age, years	41	36	62	67	82	80
Body mass index, kg/m ²	25.72	24.49	26.13	22.31	31.22	36.72
Cerebral ischemia history	No	No	Yes	No	Yes	No
Chronic obstructive pulmonary disease	No	No	Yes	Yes	No	No
Autoimmune diseases	No	No	No	No	No	Yes
Diabetes	No	No	No	No	No	Yes
Chronic kidney diseases	Yes	No	No	No	No	No
Hypertension	No	No	No	No	Yes	Yes
Diagnostics	Polymerase chain reaction (PCR)					

Table 2: Exo-miRNA name, fold change (FC)^a, p-values, and 95% confidence interval (CI) values are provided.

Exo-miRNA	FC ^a	p-Value (t-test)	p-adju (BH)	ACE+ 95% CI	ACE- 95% CI
Hsa-let-7g-5p	2.148148148	0.005070939	0.23803582	4.202–4.362	5.198–13.362
Hsa-miR-208a-3p	0.490723211	0.00484839	0.27635825	5.151–12.456	4.165–4.361
Hsa-miR-323a-3p	0.438652902	0.000535342	0.21360128	6.989–12.707	4.162–4.361
Hsa-miR-4454+hsa-miR-7975	2.645447531	0.001011331	0.26901412	4.141–4.315	7.267–15.589

^aExoACE2-expressing divided by non ACE2-expressing. p-Value refers to the difference between two groups obtained by t-test. The adjusted p-value following the Benjamini–Hochberg (BH) procedure is also shown.

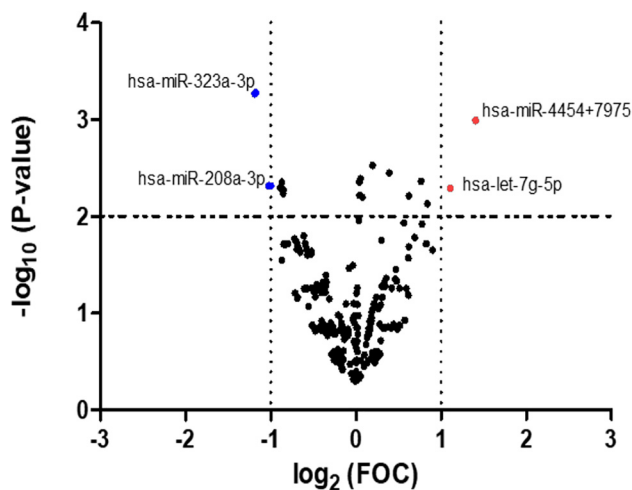


Figure 4: Volcano plot of the differentially expressed exo-miRNAs as assessed by a microarray analysis in serum exosomes from COVID-19 patients sorted by ACE2 presence/absence. The y-axis indicates the $-\log_{10}$ of the p-values and the x-axis is the fold change (FOC) measured as the \log_2 -transformed ratio of the expression between both experimental groups.

and critical reading, Prof. Donato Cosco for his technical assistance.

Research funding: The study was partially supported by Calabria Region (no. COVID19@UMG POR Calabria-FESR/FSE 2014–2020 D.D.R.C. n. 4584 del 4/5/2021- Azione 10.5.12).

Author contributions: S.M. and E.I. designed and conducted the research, analyzed the data, wrote the manuscript and supervised the work; A.M.Z. conducted the research and analyzed the data; S.R. and C.T. supervised the clinical aspect of the research and provided the biological samples; E.C. conducted the NanoString analysis; N.N., A.A., helped in the exosomes purification and RNA purification; D.M. and V.D. helped in the data analysis and in the revision of manuscript; A.M.T. performed the physical characterization of exosomes; R.L., A.R. and E.M.T. helped following the clinical aspect of the research; A.Q., G.T. and N.M. helped in biological samples storage, serum purification and analysis, A.F., A.D.L., revised the manuscript and followed the conceptualization. All authors read and approved the final manuscript. All authors have accepted responsibility for the entire content of this manuscript and approved its submission.

Competing interests: Authors state no conflict of interest.

Informed consent: Written informed consent was obtained from all the participants before blood samples collection for the purpose of this study.

Ethical approval: The study was conducted according to the standards of the Declaration of Helsinki (revised in 2008) [World Medical 2013], was approved by the ethical committee and was partially supported by Calabria Region (no. COVID19@UMG POR Calabria-FESR/FSE 2014–2020 D.D.R.C. n. 4584 del 4/5/2021- Azione 10.5.12).

References

- Del Rio C, Malani PN. COVID-19 in 2022—the beginning of the end or the end of the beginning? *JAMA* 2022;327:2389–90.
- El-Shennawy L, Hoffmann AD, Dashzeveg NK, McAndrews KM, Mehl PJ, Cornish D, et al. Circulating ACE2-expressing extracellular vesicles block broad strains of SARS-CoV-2. *Nat Commun* 2022;13:405.
- Yu D, Li Y, Wang M, Gu J, Xu W, Cai H, et al. Exosomes as a new Frontier of cancer liquid biopsy. *Mol Cancer* 2022;21:56.
- Kalluri R, LeBleu VS. The biology, function, and biomedical applications of exosomes. *Science* 2020;367:eaau6977.
- Li S, Yi M, Dong B, Tan X, Luo S, Wu K. The role of exosomes in liquid biopsy for cancer diagnosis and prognosis prediction. *Int J Cancer* 2021; 148:2640–51.
- Lopez-Verrilli MA, Court FA. Exosomes: mediators of communication in eukaryotes. *Biol Res* 2013;46:5–11.
- Zhang L, Yu D. Exosomes in cancer development, metastasis, and immunity. *Biochim Biophys Acta Rev Cancer* 2019;1871:455–68.
- Wood H. Exosomal microRNAs may aid differential diagnosis of movement disorders. *Nat Rev Neurol* 2022;18:1.
- Tkach M, Kowal J, Théry C. Why the need and how to approach the functional diversity of extracellular vesicles. *Philos Trans R Soc Lond B Biol Sci* 2018;373:20160479.
- Ludwig N, Whiteside TL, Reichert TE. Challenges in exosome isolation and analysis in health and disease. *Int J Mol Sci* 2019;20:4684.
- Kowal EJK, Ter-Ovanesyan D, Regev A, Church GM. Extracellular vesicle isolation and analysis by western blotting. *Methods Mol Biol* 2017;1660: 143–52.
- Iaccino E, Mimmi S, Dattilo V, Marino F, Candeloro P, Di Loria A, et al. Monitoring multiple myeloma by idiotype-specific peptide binders of tumor-derived exosomes. *Mol Cancer* 2017;16:159.
- Maisano D, Mimmi S, Dattilo V, Marino F, Gentile M, Vecchio E, et al. A novel phage display based platform for exosome diversity characterization. *Nanoscale* 2022;14:2998–3003.
- Noonin C, Thongboonkerd V. Exosome-inflammasome crosstalk and their roles in inflammatory responses. *Theranostics* 2021;11:4436–51.
- Zhang J, Li S, Li L, Li M, Guo C, Yao J, et al. Exosome and exosomal microRNA: trafficking, sorting, and function. *Genomics Proteomics Bioinf* 2015;13:17–24.
- Piao XM, Cha EJ, Yun SJ, Kim WJ. Role of exosomal miRNA in bladder cancer: a promising liquid biopsy biomarker. *Int J Mol Sci* 2021;22: 1713.
- Manna I, Quattrone A, De Benedittis S, Vescio B, Iaccino E, Quattrone A. Exosomal miRNA as peripheral biomarkers in Parkinson's disease and progressive supranuclear palsy: a pilot study. *Parkinsonism Relat Disord* 2021;93:77–84.
- Théry C, Witwer KW, Aikawa E, Alcaraz MJ, Anderson JD, Andriantsitohaina R, et al. Minimal information for studies of extracellular vesicles 2018 (MISEV2018): a position statement of the International Society for Extracellular Vesicles and update of the MISEV2014 guidelines. *J Extracell Vesicles* 2018; 7:1535750.
- Wells AC, Daniels KA, Angelou CC, Fagerberg E, Burnside AS, Markstein M, et al. Modulation of let-7 miRNAs controls the differentiation of effector CD8 T cells. *Elife* 2017;6:e26398.
- Letafati A, Najafi S, Mottahedi M, Karimzadeh M, Shahini A, Garousi S, et al. MicroRNA let-7 and viral infections: focus on mechanisms of action. *Cell Mol Biol Lett* 2022;27:14.
- Fernández-Pato A, Virseda-Berdecies A, Resino S, Ryan P, Martínez-González O, Pérez-García F, et al. Plasma miRNA profile at COVID-19 onset predicts severity status and mortality. *Emerging Microbes Infect* 2022;11:676–88.
- Latini A, Vancheri C, Amati F, Morini E, Grelli S, Claudia M, et al. Expression analysis of miRNA hsa-let7b-5p in naso-oropharyngeal swabs of COVID-19 patients supports its role in regulating ACE2 and DPP4 receptors. *J Cell Mol Med* 2022;26:4940–8.
- Bi S, Wang C, Jin Y, Lv Z, Xing X, Lu Q. Correlation between serum exosome derived miR208a and acute coronary syndrome. *Int J Clin Exp Med* 2015;8:4275–80.
- Garg A, Seeliger B, Derda AA, Xiao K, Gietz A, Scherf K, et al. Circulating cardiovascular microRNAs in critically ill COVID-19 patients. *Eur J Heart Failure* 2021;23:468–75.